Spectrochimica Acta Part A: Molecular and Biomolecular Spectroscopy 241 (2020) 118682

Contents lists available at ScienceDirect

Spectrochimica Acta Part A: Molecular and Biomolecular Spectroscopy

journal homepage: www.elsevier.com/locate/saa

Mercuric ion detection by plasmon-enhanced spectrophotometric ellipsometer using specific oligonucleotide probes

Mustafa Oguzhan Caglayan

Bilecik Seyh Edebali University, Faculty of Engineering, Bioengineering Department, Bilecik, Turkiye

ARTICLE INFO

Article history:
Received 3 January 2020
Received in revised form 18 June 2020
Accepted 30 June 2020
Available online 2 July 2020

Keywords:
Mercuric ion
Biosensor
Surface plasmon resonance
Total internal reflection
Spectrophotometric ellipsometry
Mercury specific oligonucleotide probes

ABSTRACT

Pollution due to heavy metal ions, including mercury, has become a major issue because of their toxicities. It is required to monitor mercury levels in aqueous media using fast and selective methods with high accuracy. Ellipsometry is a promising technique for instance when it's combined with the plasmon resonance phenomena. We reported a biosensor system available for qualitative/quantitative determination of mercuric ions in aqueous media where both the spectrophotometric ellipsometry and oligonucleotide recognition elements were used. A single step assay using both a linear (ProbeL) and a hair-pin (ProbeH) type oligonucleotide probe as a recognition element, in addition to a sandwich-type (ProbeLS) assay were developed and compared. The detection limits were 0.23 nM, 0.03 nM and 0.15 pM for ProbeL, ProbeH and ProbeLS, respectively. The detection range was between 0.05 nM and 100 nM Hg^{2+} for all assays proposed herein.

1. Introduction

The mercuric ion (Hg^{2+}) is an environmental pollutant with very high toxicity and is a substance with fatal effects on human health in the form of brain, kidney and many other organ damages [1–3]. The microbial methylation of mercuric ion results in a potential neurotoxic agent, methylated mercury, that passes through the food chain from the tissues of fish and marine mammals [4]. These compounds are readily consumed by bacteria, plankton, fish, and accumulate throughout the biological cycle and increase their concentration [5]. In addition, studies have shown that many aquatic environments destroy viable cell activity [6] and damage proliferation by energy metabolism. For this reason, it is crucial to determine Hg^{2+} ions in aqueous media both for environmental and health issues [7]. The continuous and routine control of Hg^{2+} in rivers and large water basins is used to determine the safety of foodstuffs supplied from water. Thus, it is desirable to develop a precise mercury detection method that is simple, practical and suitable for routinely performing Hg^{2+} determination on a large number of samples in both environmental and water samples.

There are various methods for Hg^{2+} monitoring/detection such as polarography, atomic absorption, atomic emission, fluorescence spectrometry, inductively coupled plasma (ICP) spectrometry and ICP-mass spectrometry [8]. However, although these methods have analytical advantages, they also have some disadvantages such as their requirements for high amounts of aliquots, long-time processing, a very good chemistry and instrumentation knowledge, and expensive equipment [9].

Consequently, there are various methods for mercuric ion detection and monitoring reported in the literature. Colorimetric [10–15], fluorescence based [16–20], electrochemical [18,21–23] and plasmonic [24–26] methods were reported to detect this pollutant with faster and relatively selective method. There are a number of reviews on the Hg^{2+} detection/monitoring techniques in the literature which is quite versatile to learn about the state of the art [4,23,24,27–30].

In this work, we discuss the analytic performance of spectrophotometric ellipsometry which is a refractive method and its combination with surface plasmon resonance (SPR) conditions (Fig. 1a). Both the SPR and spectrophotometric ellipsometry can be used for the analysis and the characterization of ultra-thin films deposited on any reflective (but smooth) surfaces in physics, chemistry and biology fields. The incorporation of these techniques depends on the design of the appropriate sensor chip and immobilization techniques [31–33]. In SPR based sensor applications, the detection limit can be reduced to 10 nM oligonucleotide target [34]. Another advantage of this method is that less than 500 μL of sample is used for an assay. Ellipsometry applications are usually used when the thin films are characterized [35,36]. However, it is possible to carry out analysis in the solution medium and under conditions of total internal reflection ellipsometry (TIRE). Our group has developed a number of TIRE sensors for various targets and recognition elements, such as oligonucleotide based *M. tuberculosis*

E-mail address: oguzhan.caglayan@bilecik.edu.tr.

https://doi.org/10.1016/j.saa.2020.118682
1386-1425/

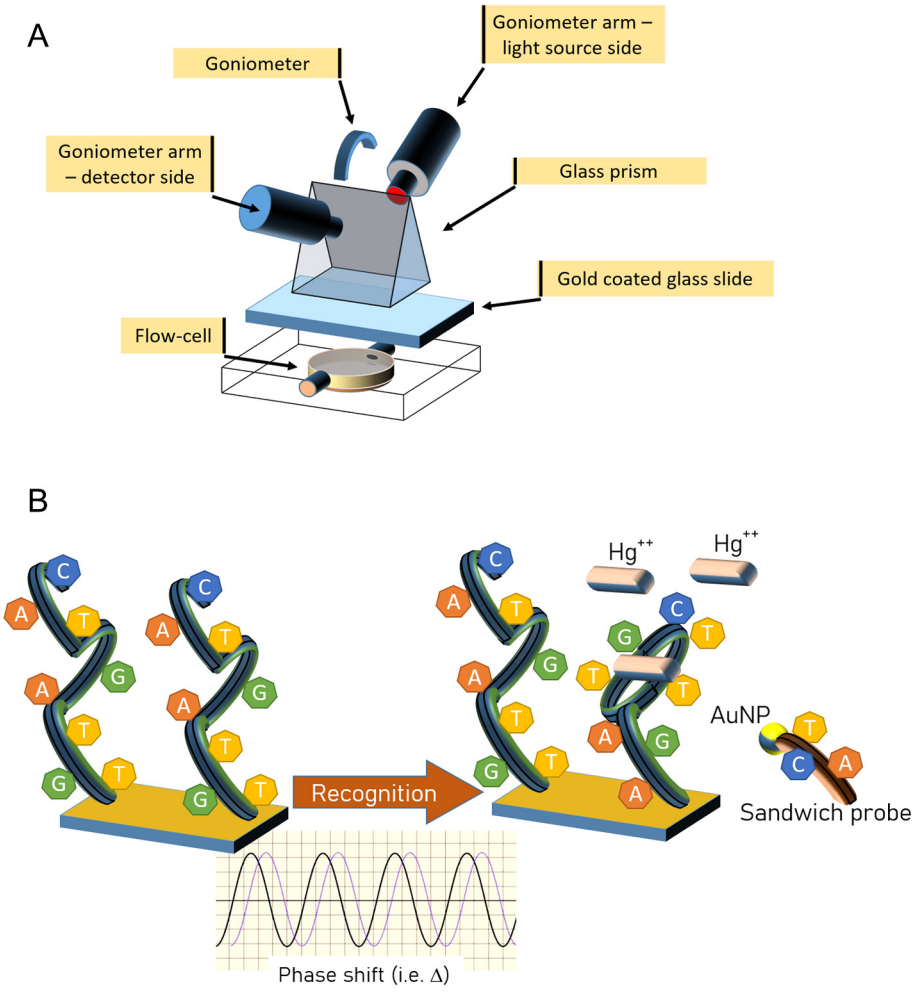

Fig. 1. a) Schematic diagram of spectrophotometric ellipsometry method under SPR conditions. b) Schematic representation of oligonucleotide probe based analysis and sensor response upon target molecule binding.

[34] and avian influenza A [37] sensor, RNA aptamer for HIV-tat protein detection [38], aptamer based Hg^{2+} [39] and zearalenone toxin detection [40], and heavy metal detection [41].

Determination of a particular heavy metal ion by an optical-based method such as refractive methods (e.g. SPR) is difficult because metal ions have similar refraction index values and are permeable in a dilute form. For this reason, the studies made are relating to the preparation of surfaces that are specific to certain heavy metals and the application of SPR techniques on these surfaces. For instance, 1,6-hexane dithiol has been used for selectively adsorbing Hg^{2+} ion [42] in a SPR sensor with limit of detection (LOD) of 100 μM. In a study using cross-linked chitosan which is also a good adsorbent for heavy metals due to a large number of amino groups on it [43], 500 ppb Hg^{2+} LOD has been reported. Yu and coworkers [44] reported a Hg^{2+} specific surface where both polypyrrole and 2-mercapto benzothiazole were used for selectivity, with a LOD of 10 ppb. In another study where polypyrrole-chitosan polymer composites have been used, 50 ppb LOD was reported but selectivity was poor against to Pb^{2+} ions [45].

Another approach to the identification of mercury ions is the use of DNA probes. The selectivity of thymine-Hg^{2+}-thymine complexes have been reported earlier by Katz in 1963 [46]. Furthermore, higher stability of this complex than A-T base pair has also been reported [47]. It is also known that the thymine-thymine (TT) mismatch formed in this manner is more specific to Hg^{2+} than to other metal ions such as Ag^{+}, Cu^{2+}, Ni^{2+}, Pd^{2+}, Co^{2+}, Mn^{2+}, Pb^{2+}, Cd^{2+}, Mg^{2+}, Ca^{2+}, Fe^{2+}, Fe^{3+} and Ru^{3+} [48]. Due to this specificity, too much work has been done to determine the mercury ion on the Hg^{2+} binding with the TT mismatch. Different detection methods such as fluorescence resonance energy transfer technique [49], colorimetric sensors [50], electrochemical detection [51] and DNA-enzyme based sensors [52] techniques have been reported.

Researchers are more interested in the hairpin DNA structures for sensor applications, since their sensitivity, detection capacity, and stability are more than linear DNA structures as a signal-recognition element [53]. We preferred this structure because this may provide a higher signal in the determination of targets due to dense formation possibility in the vicinity of plasmon wave. An Hg^{2+} ion assay was performed under SPR conditions using hair-pin DNA probe has been reported with the detection range for the Hg^{2+} ion from 5 nM to 5000 nM and 5 nM LOD [54].

In this study, SPR and TIRE methods were combined to increase the response from the TIRE sensor and reduce the detection limit for Hg^{2+} with the aid of the SPR phenomenon. Moreover, to compare the effect of probe type to the analytical performance herein, three different probes were used in this study. Two of the probes were used for direct assay, where their structural formation was different (linear and hairpin) while another probe was used for a sandwich assay using gold nanoparticles to further signal improvement (Fig. 1b).

2. Materials and methods

2.1. General

Except otherwise stated, instruments and chemicals used in the study are as follows: Ellipsometer (TT40 Spectrophotometric ellipsometer, China), TIRE flow system (custom made), BK7 prism and immersion oils (ThorLabs, Germany), Atomic Force Microscope (ParkSystem XE100, Korea) Femtoscience, Korea), Spectrophotometer (Shimadzu 1601, Japan), all chemical substances (Sigma-Aldrich, Merck or Alfa-Aesar, analytical grade or higher purity), oligonucleotides (Heliksbio, Turkey), distilled water (Millipore-Q, USA, 18 MΩ).

2.2. SPR condition

The SPR condition was provided by a definite thickness ultra-thin metal film (Au) coated glass slide where SPR phenomena is computable for a given wavelength and angle of incidence. Glass slides with these properties (BK7, refraction index at 532 nm is 1.58 at 25 °C) were used. Aggressive oxidant treatment with 4:1 (by volume) concentrated sulfuric acid and hydrogen peroxide solution then cleaning with a plasma device (Femtoscience, Korea) under an air plasma of 100 W for 30 min, followed by washing with ethyl alcohol/acetone was the standard cleaning procedure prior to any modification. Metal coating was done to achieve an adhesive layer (3 nm Cr) under the Au layer (52 nm) on the substrate by physical vapor deposition. Au-plated SPRe-TIRE chips were used after cleaning with the plasma device for 20 min before immobilization.

2.3. Probe immobilization

The Hg-specific oligonucleotide sequences (ProbL, ProbeH and ProbeLS, Table 1) containing the SH terminated end were immobilized on the gold surface using the self-assembly approach. The immobilization conditions for the probes were determined by ellipsometric thickness measurements at each immobilization step. The solution containing probe prepared in PBS (pH 7.3) buffer at concentrations between 0.5 nM and 10 μM was used to determine optimal probe immobilization conditions. The immobilizations were carried out at room temperature for 1–6 h in a dark environment. After the interaction, the surface film thickness of the sensor surface was measured ellipsometrically (model parameters selected from the library of the equipment are BK7/Au/Organic layer). Mercaptohexanol (MCH), prepared in PBS buffer at a concentration of 100 μM prior to each run, was conjugated to the surface.

The sandwich-structured analysis was performed using a secondary complementary single strand oligonucleotide probe obtained by modifying the gold nanoparticle (AuNP) to increase the signal from the SPRe-TIRE sensor. First, the Hg^{2+} specific oligonucleotide ProbLS sequence was immobilized on the Au-coated surface. The immobilization conditions were optimized again, because of differences in sequences and variation in the number of bases. The ProbLS solution (5.0 nM - 5.0 μM) prepared in PBS buffer was interacted with the surface at room temperature in a dark environment for 6 h. The measured ellipsometric thickness variation after surface immobilization of ProbLS, at different concentrations, is listed in Supplementary Section in Table S1. The optimal concentration in the PBS buffer for ProbeLS immobilization was determined to be 0.75 μM. The sensor surface after ProbLS immobilization was also blocked with the MCH prepared in PBS buffer (100 μM).

AuNPs were synthesized from auric acid (~40 nm) by citrate reduction method. Then, complementary probe for sandwich assay (CSS) was immobilized on AuNPs. For this purpose, 1 mM, 10 mL of aqueous auric acid solution was reduced using 1 mL of 38.8 mM trisodium citrate dihydrate solution. Under continuous stirring, the hot citric acid solution was poured dropwise into auric acid solution at the room temperature. AuNPs were obtained in solution in the colloidal state. The colloidal solution was then centrifuged under cooled-ultracentrifuge and washed using absolute ethyl alcohol, repeatedly. Then CSS at concentrations from 1 nM to 1000 nM (in PBS) was allowed to interaction for immobilization. At this step, the conjugation was monitored using UV–vis Spectrophotometer at 528 nm, and 10 min of interaction was deemed to be adequate for the completion of the conjugation between the probe and the AuNP. The AuNP concentration was also optimized for conjugation for 10 min (see Table S2), and, then, all CSSs were prepared using 500 nM AuNPs in PBS buffer.

Table 1
ODN probe sequences used in the study.

ODN sequence	Description
5′-SH-$(A)_{20}$- TTCGT GTTGT GTTCG-3′	ProbL
5′-SH-$(CH_2)_6$- CGGGG GACAG GACTT GACCT TCTCC GCCTT CTTCT CTCCT GTCCC CCG-3′	ProbH (Hair-pin)
5′-SH-$(CH_2)_6$- ATTCT TTCTT CCCCC CGGTT GTTTG TTT- 3′	ProbLS (Sandwich assay – probe immobilized probe surface)
5′-SH- AAACA AACAA-3′	Complementary sequence (Sandwich assay)

2.4. Spectrophotometric ellipsometry under SPR condition

After immobilization of ProbH, ProbL, ProbLS and the blocking agent MCH at appropriate conditions, analytical performance of the assay was tested for Hg^{2+} determination in aqueous media. For this purpose, the kinetic data were obtained by using an ellipsometer. In the TIRE configuration, ellipsometric angles Δ (Delta) and Ψ (Psi) were measured real-time (by 2–4 s intervals). When Hg^{2+} binds to the probe, refractive index and extinction of the interface (i.e. n and k) are changed that, in turn, results in a time-dependent change of Δ (phase shift) angle. The Δ is more vulnerable to the interface refractive index changes when it is at/near SPR conditions where the phase shift has nearly infinite slope. Furthermore, to determine the specificity of the ProbeLS, $PbCl_2$ solution prepared in PBS buffer (10 nM) was also used. From the kinetic data obtained, the range of detection and limit of detection of the assays were calculated and reported.

3. Results and discussion

3.1. Analytic performances of direct assays

The sensor response of probes ProbH and ProbL immobilized sensor chips to Hg^{2+} at different concentrations (0.05 nM to 100 nM) was investigated. The kinetic data of both probes acquired during the sensor surface-immobilization showed the surface saturation is achieved at 600 s (10 min) at room temperature. The main advantage of such a biosensor system is that the analysis time is limited to a period of 10 min. The probe responses of ProbL and ProbH are compared in Table S3. In the first 100 s, at low Hg^{2+} concentrations, 90% of the total sensor response was reached, but, at higher concentrations, it dropped to around 50%, which possibly indicates a non-favorable kinetics. Moreover, the standard deviations reported in this table are probably as a result of realtime-kinetic measurements using microfluidic cell (e.g. due to the micro-temperature changes), because, under appropriate conditions, the Δ measurement accuracy of the ellipsometer is ±0.0001° (degree). Also, the ProbH sensor response was significantly higher than that of ProbL sensor. Although the sensor response obtained for the ProbL is low compared to other probes while comparing the detection limit, the accuracy of ProbL sensor is good in terms of standard deviations listed in the table. Furthermore, for the hairpin oligonucleotide, the structural formation change that occurred upon Hg^{2+} binding also largely changed the ellipsometric angle, delta. In fact, the ellipsometer is a device sensitive to the surface deposited material thickness (for a

material with definite refractive index and extinction coefficient). For this reason, both the Hg^{2+} binding and the structural formation change cause a very high sensor signal in comparison with the other probes.

In Fig. 2, the sensor response versus the log Hg^{2+} concentration for ProbL and ProbH is shown, respectively, in other words, the sensor calibration graph.

For the measurements performed for ProbH and ProbL, the maximum standard deviations (σ) were calculated as 0.231° and 0.251°, respectively. The detection limit (LOD) calculated from the calibration curves for 3σ was 0.0395 nM for ProbH and 0.232 nM for ProbL. Also, taking into account the calibration curves, the detection sensitivity for the ProbH (in other words, the slope of the calibration curve) is about 3.5 times higher when compared to ProbL. No surprise is observed in the selectivity study with Pb^{2+}, since the thymine-Hg^{2+}-thymine interaction is extremely specific [55]. The Pb^{2+} signal obtained for ProbL and ProbH probes were within the noise range (3σ) of the assay.

3.2. Analytic performance of sandwich assay

The sandwich assay was performed using secondary conjugated oligonucleotide probe obtained by modifying the gold nanoparticle (AuNP) to increase the signal to be received from SPRe-TIRE sensor. The UV spectrophotometer analysis showed that the localized plasmon resonance peak observed at 528 nm. In this case, the approximate size of the nanoparticles obtained can be said to be around 40 nm. The interaction of the AuNP-conjugate pair with the ProbLS, which was previously immobilized on the surface and bound to Hg^{2+}, resulted in a rapid increase for the sensor response. It was thought that this rapid increase was caused by sudden agglomeration of sandwich pair resulted in a sudden refractive index and thickness changes. Then, the PBS buffer was used to remove the unbound AuNP-conjugate pair, and, in turn, the unbound AuNP-conjugate pairs were removed from the surface. After getting a steady increasing sensor response, the calibration graph is constructed using sensor response at 20th minute.

The sensor calibration graph is shown in Fig. 3. The sandwich sensor gives a low slope but high cut-off (i.e. high detection limit but low sensitivity) as AuNP changes the surface ellipsometric parameters excessively due to its 40 nm size. The detection limit for this sensor, which was calculated for 3σ as in the previous section, was 0.15 pM since the maximum σ is 0.219 for this assay. The detection sensitivity (i.e. slope) was smaller than that of ProbH and greater than that of ProbL.

3.3. Comparison of sensor types

The sensor sensitivities (i.e. slope of the calibration curve) and the calculated detection limits (i.e. using 3σ) for ProbH, ProbL and ProbLS used in the study are given in Table 2.

ProbL gives the lowest value in terms of both sensitivity and detection limit and shows suitable results for SPRe-TIRE performance in terms of analytical limit. For instance, a 5 nM LOD has been reported by two researchers in a SPR assay [54,56]. It is expected that TIRE performance will frequently be better than the results obtained in SPR analysis, since the SPR is sensitive only to the refractive index and examines the change in light intensity in only one plane of polarized light. For this reason, SPR sensors cannot provide the accuracy and sensitivity of an ellipsometer with TIRE configuration.

In particular, ProbH can be an important quantitative sensor alternative, as it offers a detection limit of about 40 pM Hg^{2+} (in PBS buffer) and is highly sensitive. However, with a detection limit of about 0.1 pM, ProbLS (i.e. sandwich analysis) can be very successful in the presence/absence analysis, but the quantification ability (i.e. sensitivity) is about 60% less than that of the ProbH assay. In addition, it was observed that the proposed linear and hairpin probe yields higher analytical

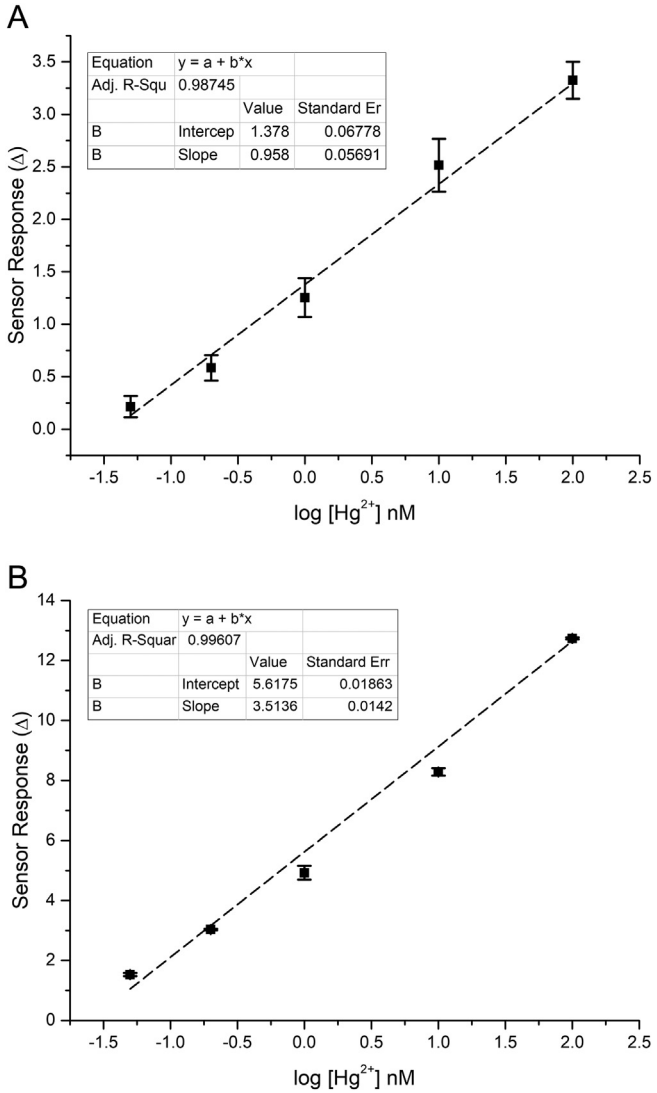

Fig. 2. ProbL (a) and ProbH (b) sensor calibration curve for 0.05 nM to 100 nM Hg^{2+}. The change in sensor response Δ is given in degrees. Standard deviations were calculated for 4 replicates in series.

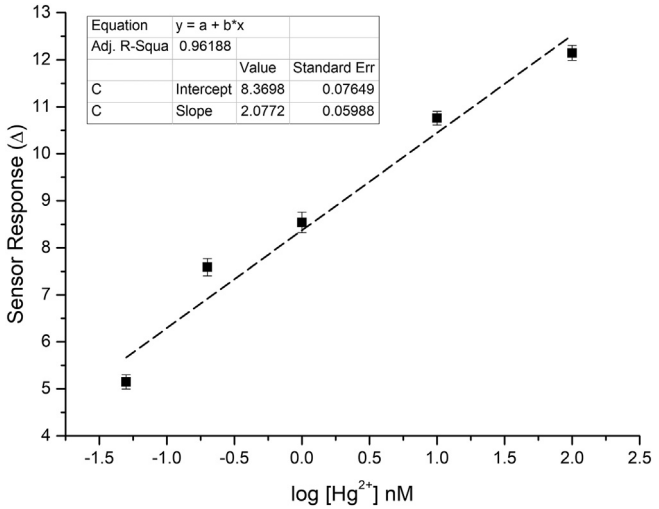

Fig. 3. ProbLS sandwich analysis sensor calibration curve for 0.05–100 nM Hg^{2+}. The change in sensor response Δ is given in degrees. The standard deviations were calculated for 4 replicates in series.

Table 2
Comparison of sensor analytical performance parameters obtained from the calibration curves of the sensors.

Sensor type	Slope	Std error	Intercept	Std error	Calculated detection limit pM Hg^{2+}
ProbL	0.9584	0.0569	1.3780	0.0678	232
ProbH	3.5136	0.0142	5.6175	0.0186	39.5
ProbLS	2.0772	0.0599	8.3698	0.0765	0.15

performance than colorimetric and fluorometric strategies compared to some literature examples given in Table 3. However, in an electrochemical sensor study using the hairpin probe [22], a slightly better analytical performance was reported than ProbeH. Unfortunately, no comparison can be made regarding the use of optic sensors for hairpin structures. However, compared to the studies reporting the sandwich analysis approach (or the use of AuNP for signal enhancement purposes), it showed better analytical performance compared to most sensors listed in Table 3. However, the analytical performance of ProbeLS was rather low compared to the electrochemical sensor using only electrodeposited graphene and AuNP [62]. As expected, the ProbLS array provided a LOD 2800 times lower than ProbL and 400 times lower than ProbH.

4. Conclusions

In this study, SPReTIRE based biosensor with three different configurations has been developed for the determination of Hg^{2+} in aqueous media. The direct analysis using linear (ProbL) and hairpin (ProbH) probes, in addition to a sandwich assay (ProbLS and AuNP-conjugate), were used. The LOD for the Hg^{2+} solution prepared in PBS buffer reached 0.15 pM in the sandwich analysis which is quite well when compared with the literature reports. The specificity tests were performed using Pb^{2+} for each assay and sensor signals remained below the noise in each case. In particular, ProbH yields very good results both in terms of detection limit and detection accuracy.

CRediT authorship contribution statement

Mustafa Oguzhan Caglayan: Conceptualization, Data curation, Formal analysis, Funding acquisition, Investigation, Methodology, Project administration, Resources, Software, Supervision, Validation, Visualization, Writing - original draft, Writing - review & editing.

Declaration of competing interest

The authors declare that they have no known competing financial interests or personal relationships that could have appeared to influence the work reported in this paper.

Acknowledgements

This work was supported by the Scientific and Technological Research Council of Turkey (TÜBİTAK), Grant No: 112M563.

Appendix A. Supplementary data

Supplementary data to this article can be found online at https://doi.org/10.1016/j.saa.2020.118682.

References

[1] D.T. Waite, A.D. Snihura, Y. Liu, G.H. Huang, Uptake of atmospheric mercury by deionized water and aqueous solutions of inorganic salts at acidic, neutral and alkaline pH, Chemosphere 49 (2002) 341–351.
[2] N.G. Sathawara, D.J. Parikh, Y.K. Agarwal, Essential heavy metals in environmental samples from Western India, Bull. Environ. Contam. Toxicol. 73 (2004) 756–761.
[3] H.H. Harris, I.J. Pickering, G.N. George, The chemical form of mercury in fish, Science 301 (2003) 1203.
[4] T.W. Clarkson, L. Magos, G.J. Myers, The toxicology of mercury—current exposures and clinical manifestations, N. Engl. J. Med. 349 (2003) 1731–1737.
[5] R. Dragone, C. Frazzoli, C. Grappelli, L. Campanella, A new respirometric endpoint-based biosensor to assess the relative toxicity of chemicals on immobilized human cells, Ecotoxicol. Environ. Saf. 72 (2009) 273–279.
[6] A. Fanous, W. Weiss, A. Gorg, F. Jacob, H. Parlar, A proteome analysis of the cadmium and mercury response in Corynebacterium glutamicum, Proteomics 8 (2008) 4976–4986.
[7] M.C. Aragoni, M. Arca, F. Demartin, F.A. Devillanova, F. Isaia, A. Garau, V. Lippolis, F. Jalali, U. Papke, M. Shamsipur, L. Tei, A. Yari, G. Verani, Fluorometric chemosensors. Interaction of toxic heavy metal ions Pb(II), Cd(II), and Hg(II) with novel mixed-donor phenanthroline-containing macrocycles: spectrofluorometric, conductometric, and crystallographic studies, Inorg. Chem. 41 (2002) 6623–6632.
[8] S.K. Patil, D. Das, A novel rhodamine-based optical probe for mercury(II) ion in aqueous medium: a nanomolar detection, wide pH range and real water sample application, Spectrochim. Acta A Mol. Biomol. Spectrosc. 225 (2020) 117504.
[9] J. Hua, J. Yang, Y. Zhu, C. Zhao, Y. Yang, Highly fluorescent carbon quantum dots as nanoprobes for sensitive and selective determination of mercury (II) in surface waters, Spectrochim. Acta A Mol. Biomol. Spectrosc. 187 (2017) 149–155.
[10] J.-S. Lee, M.S. Han, C.A. Mirkin, Colorimetric detection of mercuric ion (Hg2+) in aqueous media using DNA-functionalized gold nanoparticles, Angew. Chem. Int. Ed. 46 (2007) 4093–4096.
[11] C.-W. Liu, Y.-T. Hsieh, C.-C. Huang, Z.-H. Lin, H.-T. Chang, Detection of mercury(ii) based on Hg2+-DNA complexes inducing the aggregation of gold nanoparticles, Chem. Commun. (2008) 2242–2244.

Table 3
Some T-T mismatch, oligonucleotide based Hg2+ detection methods reported in the literature.

Method	Approach	LOD/LOQ	Range	References
Colorimetric	AuNPs	60 nM	0.1–10 μM	[13]
Colorimetric	AuNPs	500 nM	0.1–1 μM	[55]
Colorimetric	AuNPs	0.6 nM	1 nM–100 μM	[57]
Colorimetric	Rolling circle amplification	1.6 nM	50–300 nM	[14]
Fluorescent	AuNPs, fluorescein	16 nM	0.02–1.0 μM	[58]
Fluorescent	Berberine	7.7 nM	100 nM–10 μM	[16]
Fluorescent	Fluorescein, aptamer beacon	4.28 nM	14.2–300 nM	[59]
Fluorescent	Ag nanoclusters	2.1 nM	6–160 nM	[19]
Electrochemical	Cuprous oxide-nano chitosan composite	0.15 nM	1–100 nM	[60]
Electrochemical	Direct immobilization on graphene	5 pM	25 pM–10 μM	[61]
Electrochemical	Dual hair-pin, immobilized on cyclic-dithiothreitol	28 pM	0.1 nM–5 μM	[22]
Electrochemical	Electrodeposited graphene and AuNP	0.001 aM	1 aM–100 nM	[62]
Surface enhanced resonance Raman scattering (SErRS)	Nanoporous gold, Cy-5 label	1 pM	100 pM–10 μM	[63]
SERS	Carboxytetramethyl-rhodamine reporter modified aptamer	5 nM	5 nM–5 μM	[64]
SERS	Au@Ag NP, microdroplet	10 pM	10 pM–1 μM	[65]
Field-effect transistor (FET)	Graphene	10 pM	10 pM–100 nM	[66]
Quartz crystal microbalance (QCM)	AuNP	240 pM	1–30 nM	[67]
SPRe-TIRE	None	232 pM	0.05–100 nM	This study
SPRe-TIRE	Hair-pin structure-none	39.5 pM	0.05–100 nM	This study
SPRe-TIRE	AuNP, sandwich assay	0.15 pM	0.05–100 nM	This study

[12] P. Jarujamrus, M. Amatatongchai, A. Thima, T. Khongrangdee, C. Mongkontong, Selective colorimetric sensors based on the monitoring of an unmodified silver nanoparticles (AgNPs) reduction for a simple and rapid determination of mercury, Spectrochim. Acta A Mol. Biomol. Spectrosc. 142 (2015) 86–93.
[13] J. Wu, L. Li, D. Zhu, P. He, Y. Fang, G. Cheng, Colorimetric assay for mercury (II) based on mercury-specific deoxyribonucleic acid-functionalized gold nanoparticles, Anal. Chim. Acta 694 (2011) 115–119.
[14] S. Wu, Q. Yu, C. He, N. Duan, Colorimetric aptasensor for the detection of mercury based on signal intensification by rolling circle amplification, Spectrochim. Acta A Mol. Biomol. Spectrosc. 224 (2020) 117387.
[15] K. Farhadi, M. Forough, R. Molaei, S. Hajizadeh, A. Rafipour, Highly selective Hg2+ colorimetric sensor using green synthesized and unmodified silver nanoparticles, Sensors Actuators B Chem. 161 (2012) 880–885.
[16] X. Song, B. Fu, Y. Lan, Y. Chen, Y. Wei, C. Dong, Label-free fluorescent aptasensor berberine-based strategy for ultrasensitive detection of Hg2+ ion, Spectrochim. Acta A Mol. Biomol. Spectrosc. 204 (2018) 301–307.
[17] J. Song, M. Huai, C. Wang, Z. Xu, Y. Zhao, Y. Ye, A new FRET ratiometric fluorescent chemosensor for Hg(2)(+) and its application in living EC 109 cells, Spectrochim. Acta A Mol. Biomol. Spectrosc. 139 (2015) 549–554.
[18] D.M. Chen, Z.F. Gao, J. Jia, N.B. Li, H.Q. Luo, A sensitive and selective electrochemical biosensor for detection of mercury(II) ions based on nicking endonuclease-assisted signal amplification, Sensors Actuators B Chem. 210 (2015) 290–296.
[19] J. Peng, J. Ling, X.-Q. Zhang, H.-P. Bai, L. Zheng, Q.-E. Cao, Z.-T. Ding, Sensitive detection of mercury and copper ions by fluorescent DNA/Ag nanoclusters in guanine-rich DNA hybridization, Spectrochim. Acta A Mol. Biomol. Spectrosc. 137 (2015) 1250–1257.
[20] H. Wang, Y. Wang, J. Jin, R. Yang, Gold nanoparticle-based colorimetric and "turn-on" fluorescent probe for mercury(II) ions in aqueous solution, Anal. Chem. 80 (2008) 9021–9028.
[21] J. Chamier, A.M. Crouch, Improved photoelectrochemical detection of mercury (II) with a TiO2-modified composite photoelectrode, Mater. Chem. Phys. 132 (2012) 10–16.
[22] J. Jia, Y. Ling, Z.F. Gao, J.L. Lei, H.Q. Luo, N.B. Li, A regenerative electrochemical biosensor for mercury(II) by using the insertion approach and dual-hairpin-based amplification, J. Hazard. Mater. 295 (2015) 63–69.
[23] M.B. Gumpu, S. Sethuraman, U.M. Krishnan, J.B.B. Rayappan, A review on detection of heavy metal ions in water – an electrochemical approach, Sensors Actuators B Chem. 213 (2015) 515–533.
[24] J. Du, L. Jiang, Q. Shao, X. Liu, R.S. Marks, J. Ma, X. Chen, Colorimetric detection of mercury ions based on plasmonic nanoparticles, Small 9 (2013) 1467–1481.
[25] C.V. Hoang, M. Oyama, O. Saito, M. Aono, T. Nagao, Monitoring the presence of ionic mercury in environmental water by plasmon-enhanced infrared spectroscopy, Sci. Rep. 3 (2013) 1175.
[26] R. Verma, B.D. Gupta, Detection of heavy metal ions in contaminated water by surface plasmon resonance based optical fibre sensor using conducting polymer and chitosan, Food Chem. 166 (2015) 568–575.
[27] L. Farzin, M. Shamsipur, S. Sheibani, A review: aptamer-based analytical strategies using the nanomaterials for environmental and human monitoring of toxic heavy metals, Talanta 174 (2017) 619–627.
[28] A. Hayat, J.L. Marty, Aptamer based electrochemical sensors for emerging environmental pollutants, Front. Chem. 2 (2014) 41.
[29] M.R. Knecht, M. Sethi, Bio-inspired colorimetric detection of Hg2+ and Pb2+ heavy metal ions using Au nanoparticles, Anal. Bioanal. Chem. 394 (2009) 33–46.
[30] X.B. Zhang, R.M. Kong, Y. Lu, Metal ion sensors based on DNAzymes and related DNA molecules, Annu Rev Anal Chem (Palo Alto, Calif) 4 (2011) 105–128.
[31] N.J. Geddes, A.S. Martin, F. Caruso, R.S. Urquhart, D.N. Furlong, J.R. Sambles, K.A. Than, J.A. Edgar, Immobilisation of IgG onto gold surfaces and its interaction with anti-IgG studied by surface plasmon resonance, J. Immunol. Methods 175 (1994) 149–160.
[32] H. Sota, Y. Hasegawa, M. Iwakura, Detection of conformational changes in an immobilized protein using surface plasmon resonance, Anal. Chem. 70 (1998) 2019–2024.
[33] M. Poksinski, H. Arwin, In situ monitoring of metal surfaces exposed to milk using total internal reflection ellipsometry, Sensors Actuators B Chem. 94 (2003) 247–252.
[34] M. Duman, M.O. Caglayan, G. Demirel, E. Piskin, Detection of mycobacterium tuberculosis complex using surface plasmon resonance based sensors carrying self-assembled nano-overlayers of probe oligonucleotide, Sens. Lett. 7 (2009) 535–542.
[35] G. Demirel, M.O. Çağlayan, B. Garipcan, M. Duman, E. Pişkin, Formation and organization of amino terminated self-assembled layers on Si(001) surface, Nanoscale Res. Lett. 2 (2007) 350.
[36] C.V. Ramana, V.H. Mudavakkat, K. Kamala Bharathi, V.V. Atuchin, L.D. Pokrovsky, V.N. Kruchinin, Enhanced optical constants of nanocrystalline yttrium oxide thin films, Appl. Phys. Lett. 98 (2011), 031905. .
[37] A. Keske, A. Atar, Iknur Üstünda, M.O. Çaglayan, Detection of influenza A by surface plasmon resonance enhanced total internal reflection ellipsometry, J. Comput. Theor. Nanosci. 11 (2014) 981–986.
[38] M.O. Caglayan, Z. Üstündağ, Spectrophotometric ellipsometry based Tat-protein RNA-aptasensor for HIV-1 diagnosis, Spectrochim. Acta A Mol. Biomol. Spectrosc. 227 (2020) 117748.
[39] M.O. Caglayan, Plasmon resonance-enhanced internal reflection ellipsometry for the trace detection of mercuric ion, Int. J. Environ. Sci. Technol. 15 (2018) 909–914.
[40] M.O. Caglayan, Z. Üstündağ, Detection of zearalenone in an aptamer assay using attenuated internal reflection ellipsometry and it's cereal sample applications, Food Chem. Toxicol. 136 (2020) 111081.
[41] Z. Üstündağ, M.O. Çağlayan, R. Güzel, E. Pişkin, A.O. Solak, A novel surface plasmon resonance enhanced total internal reflection ellipsometric application: electrochemically grafted isophthalic acid nanofilm on gold surface, Analyst 136 (2011) 1464–1471.
[42] S. Chah, J. Yi, R.N. Zare, Surface plasmon resonance analysis of aqueous mercuric ions, Sensors Actuators B Chem. 99 (2004) 216–222.
[43] Y.W. Fen, W.M. Mat Yunus, M. Moksin, Z. Talib, N. Yusof, Surface plasmon resonance optical sensor for mercury ion detection by crosslinked chitosan thin film, J. Optoelectron. Adv. Mater. 13 (2011) 273–279.
[44] J.C.C. Yu, E.P.C. Lai, S. Sadeghi, Surface plasmon resonance sensor for Hg(II) detection by binding interactions with polypyrrole and 2-mercaptobenzothiazole, Sensors Actuators B Chem. 101 (2004) 236–241.
[45] M.M. Abdi, L.C. Abdullah, A.R. Sadrolhosseini, W.M. Mat Yunus, M.M. Moksin, P.M. Tahir, Surface plasmon resonance sensing detection of mercury and lead ions based on conducting polymer composite, PLoS One 6 (2011) e24578.
[46] S. Katz, The reversible reaction of Hg (II) and double-stranded polynucleotides a step-function theory and its significance, Biochim. Biophys. Acta Specialized Sect. Nucleic Acids Relat. Subj. 68 (1963) 240–253.
[47] M. Yuan, Y. Zhu, X. Lou, C. Chen, G. Wei, M. Lan, J. Zhao, Sensitive label-free oligonucleotide-based microfluidic detection of mercury (II) ion by using exonuclease I, Biosens. Bioelectron. 31 (2012) 330–336.
[48] Y. Miyake, H. Togashi, M. Tashiro, H. Yamaguchi, S. Oda, M. Kudo, Y. Tanaka, Y. Kondo, R. Sawa, T. Fujimoto, T. Machinami, A. Ono, MercuryII-mediated formation of thymine-HgII-thymine base pairs in DNA duplexes, J. Am. Chem. Soc. 128 (2006) 2172–2173.
[49] M. Kumar, P. Zhang, Highly sensitive and selective label-free optical detection of mercuric ions using photon upconverting nanoparticles, Biosens. Bioelectron. 25 (2010) 2431–2435.
[50] E. Coronado, J.R. Galán-Mascarós, C. Martí-Gastaldo, E. Palomares, J.R. Durrant, R. Vilar, M. Gratzel, M.K. Nazeeruddin, Reversible colorimetric probes for mercury sensing, J. Am. Chem. Soc. 127 (2005) 12351–12356.
[51] Z. Zhu, Y. Su, J. Li, D. Li, J. Zhang, S. Song, Y. Zhao, G. Li, C. Fan, Highly sensitive electrochemical sensor for mercury(II) ions by using a mercury-specific oligonucleotide probe and gold nanoparticle-based amplification, Anal. Chem. 81 (2009) 7660–7666.
[52] T. Li, S. Dong, E. Wang, Label-free colorimetric detection of aqueous mercury ion (Hg2+) using Hg2+-modulated G-quadruplex-based DNAzymes, Anal. Chem. 81 (2009) 2144–2149.
[53] P.V. Riccelli, F. Merante, K.T. Leung, S. Bortolin, R.L. Zastawny, R. Janeczko, A.S. Benight, Hybridization of single-stranded DNA targets to immobilized complementary DNA probes: comparison of hairpin versus linear capture probes, Nucleic Acids Res. 29 (2001) 996–1004.
[54] C.C. Chang, S. Lin, S.C. Wei, C.Y. Chen, C.W. Lin, An amplified surface plasmon resonance "turn-on" sensor for mercury ion using gold nanoparticles, Biosens. Bioelectron. 30 (2011) 235–240.
[55] X. Liu, X. Cheng, T. Bing, C. Fang, D. Shangguan, Visual detection of Hg2+ with high selectivity using thymine modified gold nanoparticles, Anal. Sci. 26 (2010) 1169–1172.
[56] Y. Wang, F. Yang, X. Yang, Colorimetric biosensing of mercury(II) ion using unmodified gold nanoparticle probes and thrombin-binding aptamer, Biosens. Bioelectron. 25 (2010) 1994–1998.
[57] L. Li, B. Li, Y. Qi, Y. Jin, Label-free aptamer-based colorimetric detection of mercury ions in aqueous media using unmodified gold nanoparticles as colorimetric probe, Anal. Bioanal. Chem. 393 (2009) 2051–2057.
[58] D. Tan, Y. He, X. Xing, Y. Zhao, H. Tang, D. Pang, Aptamer functionalized gold nanoparticles based fluorescent probe for the detection of mercury (II) ion in aqueous solution, Talanta 113 (2013) 26–30.
[59] S.-H. Chen, Y.-S. Wang, Y.-S. Chen, X. Tang, J.-X. Cao, M.-H. Li, X.-F. Wang, Y.-F. Zhu, Y.-Q. Huang, Dual-channel detection of metallothioneins and mercury based on a mercury-mediated aptamer beacon using thymidine–mercury–thymidine complex as a quencher, Spectrochim. Acta A Mol. Biomol. Spectrosc. 151 (2015) 315–321.
[60] S. Liu, M. Kang, F. Yan, D. Peng, Y. Yang, L. He, M. Wang, S. Fang, Z. Zhang, Electrochemical DNA biosensor based on microspheres of cuprous oxide and nano-chitosan for Hg(II) detection, Electrochim. Acta 160 (2015) 64–73.
[61] Y. Zhang, J. Xie, Y. Liu, P. Pang, L. Feng, H. Wang, Z. Wu, W. Yang, Simple and signal-off electrochemical biosensor for mercury(II) based on thymine-mercury-thymine hybridization directly on graphene, Electrochim. Acta 170 (2015) 210–217.
[62] Y. Zhang, G.M. Zeng, L. Tang, J. Chen, Y. Zhu, X.X. He, Y. He, Electrochemical sensor based on electrodeposited graphene-Au modified electrode and nanoAu carrier amplified signal strategy for attomolar mercury detection, Anal. Chem. 87 (2015) 989–996.
[63] L. Zhang, H. Chang, A. Hirata, H. Wu, Q.-K. Xue, M. Chen, Nanoporous gold based optical sensor for sub-ppt detection of mercury ions, ACS Nano 7 (2013) 4595–4600.
[64] C.-I. Lee, J.-B. Choo, Selective trace analysis of mercury (II) ions in aqueous media using SERS-based aptamer sensor, Bull. Kor. Chem. Soc. 32 (2011) 2003–2007.
[65] E. Chung, R. Gao, J. Ko, N. Choi, D.W. Lim, E.K. Lee, S.I. Chang, J. Choo, Trace analysis of mercury(II) ions using aptamer-modified Au/Ag core-shell nanoparticles and SERS spectroscopy in a microdroplet channel, Lab Chip 13 (2013) 260–266.
[66] J.H. An, S.J. Park, O.S. Kwon, J. Bae, J. Jang, High-performance flexible graphene aptasensor for mercury detection in mussels, ACS Nano 7 (2013) 10563–10571.
[67] Z.M. Dong, G.C. Zhao, Quartz crystal microbalance aptasensor for sensitive detection of mercury(II) based on signal amplification with gold nanoparticles, Sensors (Basel) 12 (2012) 7080–7094.